RSC Advances

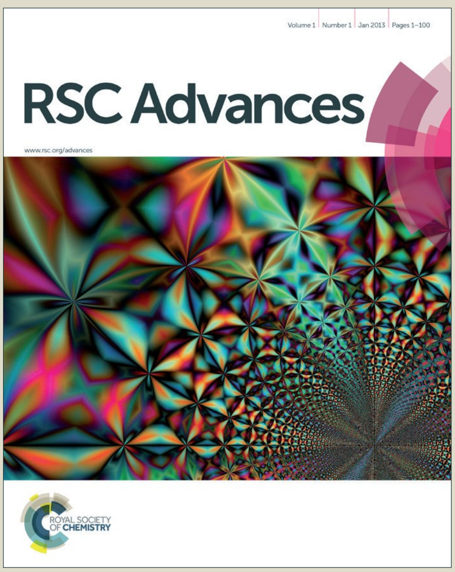

Synergetic Effect of $NbSe_2$ and Cr_2Nb on Tribological and Electrical Behavior of Cu-based Electrical Contact Composites

Qin Shi[a,b], Jin Yang[c], Wei Xiang Peng[c], Jin Ze Dong[c], Yan Qiu Chu[c], Hua Tang[c*], Chang-Sheng Li[a,c,*]

[a] School of Mechanical Engineering, Jiangsu University, 301, Xuefu Road, Zhenjiang, 212013, Jiangsu Province, P. R. China

[b] School of Mechanical Engineering, Zhenjiang Vocational Technical College, 132, Xuefu Road, Zhenjiang, 212016, Jiangsu Province, P. R. China

[c] School of Materials Science and Engineering, Jiangsu University, Key Laboratory of Tribology of Jiangsu Province, 301, Xuefu Road, Zhenjiang, 212013, Jiangsu Province, P. R. China

*Corresponding author: E-Mail: lichangsheng@ujs.edu.cn, tanghua@ujs.edu.cn, Phone: +86 511 8879 2208, Fax: +86 511 8879 2208

Abstract

The Cu-based electrical contact composites containing reinforcement (Cr_2Nb particles) and solid lubricants ($NbSe_2$ particles) were fabricated by a powder metallurgy method, and their mechanical and electrical properties were investigated. The wear tests of Cu-based composites were performed on a ball on disc under dry sliding conditions in a laboratory ambience and the worn surface of the Cu-based composites was observed by using scanning electron microscopy. Experimental results indicated that Cu-based composite materials containing Cr_2Nb and $NbSe_2$ nanofibers possessed lower electrical resistivity and better prominent tribological properties than Cu/$NbSe_2$ and Cu/Cr_2Nb composites, and that the friction coefficient and wear rate of composites gradually decreased with the increase of $NbSe_2$ nanofibers content. The lubricating effect of Cu-based composites containing 25 wt.% $NbSe_2$ nanofibers and 10 wt.% Cr_2Nb particles was outstanding with a friction coefficient close to 0.15. The tribological properties of Cu-based composites were affected by the size and morphology of $NbSe_2$ particles, and Cu-based composites with $NbSe_2$ nanofibers have been proven to be more effective to reduce friction and wear compared to Cu-based composites containing commercially available $NbSe_2$ micro-particles under dry sliding conditions. Furthermore, addition of Cr_2Nb could improve the hardness and oxidation resistance of composites, and consequently enhance wear

resistance and conductivity of Cu-based composite.

Keyword: Wear rate, Cu-based composites, Resistivity, Tribological properties

1. Introduction

Nowadays, electrical contact materials are used in every aspect of engineering applications, such as motors and generators, space shuttle, airplane, automobile, and so on. An electrical contact material with excellent performance should have high electrical and thermal conductivity, high melting point, and high resistance to environmental reaction, especially high wear resistance to maintain contact integrity. At present, copper and silver alloys [1-9] are the most widely used contact materials throughout the world. However, the application field of silver alloy is constrained to an extent because of low hardness, low strength and high cost. Copper has always attracted considerable interests owing to its high electrical and thermal conductivities, ease of production and low cost. Recently, much attention has been paid to tribological properties of Cu-based electrical contact composite materials, and intensive studies have been carried out in the past few years to enhance tribological properties of electrical contacts by appropriate addition of oxides, borides, lead, cadmium and carbides. In recent decades, various research groups have tried to enhance the tribological and mechanical properties of Cu alloy by adding of transition metal dichalcogenides (MX_2) and strengthening phase such as Cr, SiC and Cr_2Nb [10-12]. Shukla et al [13] observed that the presence of stable Cr_2Nb precipitates in Cu-based composites results in excellent retention of mechanical and electrical properties. Kumar et al [14] revealed that Cu-based composites reinforced with MoS_2 particles exhibit eminent wear resistance compared to pure copper. However, it is generally known that MoS_2 has high electrical resistance and inferior electrical conductivity. In contrast with MoS_2, although the electrical conductivity of the graphite is superior, there are serious friction and wear in vacuum or dry environments. Furthermore, the graphite and MoS_2 are more ductile, which decrease the load capacity, wear resistance properties and welding resistance of the electric contact materials. Therefore, Cu-based composites containing MoS_2 and graphite are difficult to meet the requirements such as large carrying capacity, low contact voltage and low wear loss.

Recently, attention is paid to transition metal dichalcogenides $NbSe_2$ which has a hexagonal layered structure, with the similar crystalline structure and tribological properties of MoS_2, but the electrical resistivity of $NbSe_2$ is only $10^{-4}\Omega$.cm, which is about one and six orders of magnitude lower than that of graphite and MoS_2, respectively. In previous work of our research group, we reported the fabrication and tribological properties of $NbSe_2$ nanoparticles. Zhang et al [15] prepared the uniform $NbSe_2$ nanoplates with hexagonal morphology using the facile solid state reaction method. Tang et al [16] produced single crystal $NbSe_2$ rectangular nanosheets with the simple pressureless sintered process method. Tang et al [17] reported that the copper matrix composites containing appropriate $NbSe_2$ nanofiber contents with low electrical resistivity and excellent anti-friction and wear properties will be promising for the electrical contact materials. Furthermore, since the frictional and electrical heat can be generated on a contact surface of electrical contacts, the resulting increase in temperature favors the oxidation process [18] of Cu-based composites with $NbSe_2$ nanoparticles. Oxides can lead to increase in the contact resistance and temperature, resulting in damage to the surface film and a reduction of the lubrication effect [19-20]. The high melting point intermetallic compound Cr_2Nb [21-22], which is stable and does not coarsen significantly during exposure to high temperature up to 700°C, has excellent oxidation resistance and high electrical and thermal conductivity. Therefore, the formation of fine and homogeneously distributed Cr_2Nb particles in Cu matrix not only imparts the strengthening effect of this series of composite materials but also results in enhanced mechanical properties. However, only a few relevant literatures on Cu-based composites with $NbSe_2$ nanofibers as one kind of electrical contact material are available. Furthermore, no relevant reports were found about Cu-based electrical contact composites reinforced with reinforcements of Cr_2Nb particles and solid lubricants of $NbSe_2$ nanofibers. Thus, the investigation of the effect of $NbSe_2$ and Cr_2Nb on Cu based composites is of novelty and significance.

In this study, Cu was selected as the matrix, $NbSe_2$ particles as the solid self-lubricants, and Cr_2Nb as strengthening phase. Using a simple powder metallurgy (P/M) method under non-oxidizing conditions, a production process was developed based on the concept of using the combined properties of the composites. As the main purpose of this study, the effect of $NbSe_2$ and Cr_2Nb contents on tribological properties and electrical resistivity of the composites was investigated. Furthermore, the effect of friction coefficient of Cu-based composites with commercially available $NbSe_2$ micro-particles was also investigated.

2. Materials and Methods

2.1. Fabrication of Cu-based electrical contact materials

The $NbSe_2$ nanofibers were successfully fabricated via a facile thermal solid-state reaction using micro-sized Nb and Se elements as raw materials and the details of the fabrication process was given elsewhere [23]. Furthermore, we attempted to produce the intermetallic compound Cr_2Nb [24] by a combination of mechanical alloying and thermal solid-state reaction. Full reaction of Nb with Cr could avoid the formation of Nb precipitates that are susceptible to hydrogen embrittlement. For this purpose, a slight chromium excess is sometimes preferred. After the Nb and Cr powders have been milled for 20h, a quartz ampoule which contained the milled powders (Nb powder, Cr powder) was heated at 1250°C for 1h. Subsequently the quartz was gradually cooled to room temperature, opened, and the intermetallic compound Cr_2Nb powders were obtained.

The samples of $Cu/Cr_2Nb/NbSe_2$ composites used in this study were made by powder metallurgy (P/M) and the process included a special powder treatment under non-oxidizing conditions.

Compacting and sintering of the obtained mixture were performed in protective atmosphere. The preparation process of Cu-based composites [25] included mixing, compacting, sintering and repressing. High-purity copper (150um) powders, $NbSe_2$ nanofibers and Cr_2Nb particles were mechanically alloyed in a ball mill and the milling time was 12h. The components were initially compacted at cold state in a special designed die at the pressure of 500MPa. Sintering was carried out at the temperature of 750°C in argon atmosphere for 1h. After the samples cooled to room temperature under protective atmosphere, a second pressing was performed at 500MPa. The samples were machined into a cylinder block of Φ20mm×6mm for tribo-testing experiments.

2.2. Characterization

The X-ray diffraction patterns of as-prepared powders and Cu-based composites were recorded using a D8 advance (Bruker-AXS) diffractometer with Cu Ka radiation (λ = 0.1546 nm). X-Ray photoelectron spectroscopy (XPS, Thermo ESCALAB 250Xi, USA) measurements were conducted on a instrument with an Al Kα X-ray source and samples were measured under an ultrahigh vacuum ($<10^{-9}$ mbar). The structure and morphology of the samples were characterized by optical microscope, scanning electron microscopy (SEM, JEOL JXA-840A), transmission electron microscopy (TEM, a JEOL-2010 HRTEM), and energy dispersive spectrometer. All the measurements were carried out at room temperature. Microhardness of composites was evaluated at air atmosphere by a microhardness tester with a Vickers indenter (Duramin-A300).

2.3. Tribological tests procedure

Based on existing literatures [17, 31-32], wear tests of electrical contacts were measured in ball-on-disk or pin-on-disk under two different configurations: reciprocating and rotating. The typical sliding electrical contact materials such as the commutator or collecting ring which are applied in conducting the electric currents between the fixed parts and the rotating components of generator widely, and the collecting ring or commutator slide continuously in one direction against metal matrix alloys under dry conditions. In view of the above mentioned facts, a ball on disk tribometer was used to evaluate the tribological properties of Cu-based composites in this work. A fixed disc specimen (20mm in diameter, 6mm in height) of Cu-based composite materials was rubbed against the spherical surface of a rotating ball specimen. Ball specimens (4mm in diameter) were produced from the 440C stainless steel having a hardness of 745HV. All tribological tests were performed at least four times under the same condition and the mean or maximal and minimal values are reported. Before each test experiment, the samples were abraded with 900 abrasive papers and then cleaned with acetone followed by drying. The wear volume loss and wear rate were measured as reported in a previous paper [30]. Wear track profiles were measured by a profilometer (SV-3000; Mitutoyo, Kanagawa, Japan). The wear volume loss is determined as $V=AL$, where A was the cross section area of worn scar, and L was the perimeter of worn scar. The cross section area of worn scar (A) was obtained from four independent measurements for each wear track. The wear rate $W=V/SN$ [29], was calculated as a function of the wear volume divided by the sliding distance S and the applied load N, and expressed as $mm^3N^{-1}m^{-1}$.

2.4. Electrical resistivity measurements

The electrical resistivity of Cu-based composites was measured by the D.C. four-point probe method [26]. The four-point probe method which has been proven to be a convenient tool for the electrical resistivity measurement is generally preferred for low resistance measurements. A four-point probe measurement was performed by making four electrical contacts to the sample surface. Two of the probes were used to source current and the other two probes were used to measure voltage. The measurement errors could be eliminated by using four probes due to the probe resistance, the spreading resistance under each probe, and the contact resistance between each metal probe and material. The resistance data were converted to resistivity values with the measured sample dimensions.

3. Results and discussion

3.1. Characterization of materials

The morphology and structure of the $NbSe_2$ nanofibers were characterized using SEM and TEM. Fig.1a shows thin, long threadlike $NbSe_2$ nanofibers prepared by a facile solid state reaction, the average length was up to a few microns and average diameter about 200nm. From the magnified SEM image (Fig.1b), $NbSe_2$ nanofibers had a laminar structure, and the fiber of the big size consisted of plenty of small nanofibers. Fig.1c exhibits the TEM image of $NbSe_2$ nanofibers, which was consistent with SEM observations. Fig.1d shows the [0001] zone-axis high resolution TEM (HRTEM) and the [0001] zone-axis selected area electron diffraction (SAED) of $NbSe_2$ single nanofiber (inset). It could be clearly depicted that the $NbSe_2$ nanofibers had a regular lamellar hexagonal structure, and the lattice fringe had a spacing of 0.62nm corresponding to the theoretical d–spacing for (002) planes of the hexagonal $NbSe_2$ structure. The SAED pattern in Figure 2d indicated that the nanofibers grew normally to the [0001] direction.

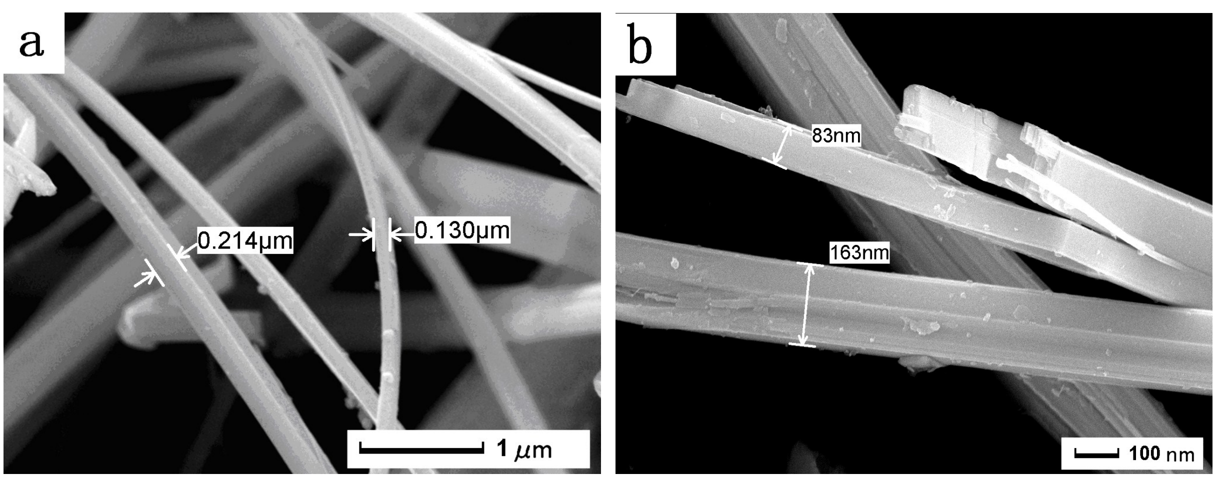

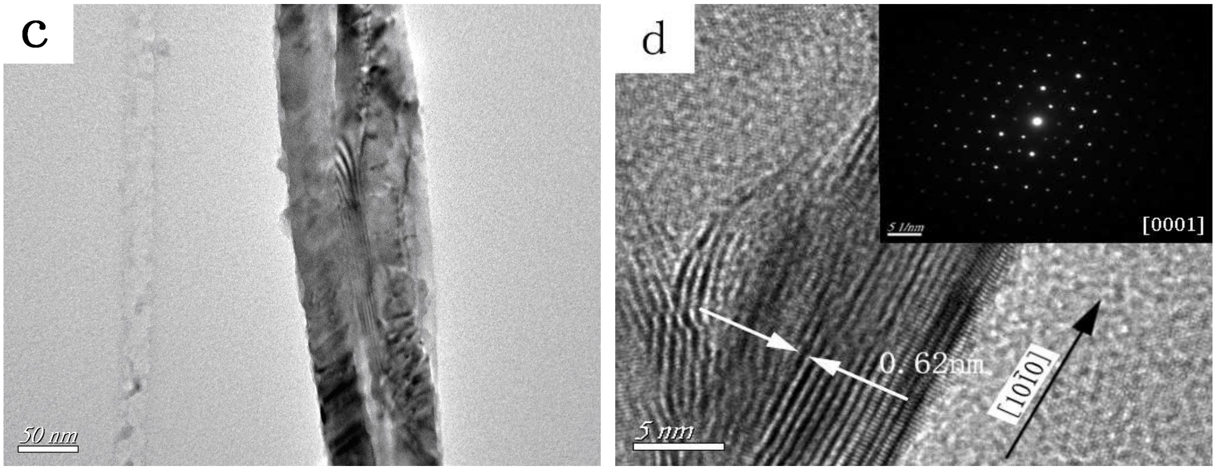

Fig.1 (a) Low magnified SEM image of $NbSe_2$ nanofibers, (b) High magnified SEM image of $NbSe_2$ nanofibers, (c) TEM image of $NbSe_2$ nanofibers, (d) HRTEM image of $NbSe_2$ nanofibers

The XRD pattern of $NbSe_2$ nanofibers is shown in Fig.2. All labeled diffraction peaks of as-prepared $NbSe_2$ could be indexed to hexagonal crystal structure, which coincided with the values of standard card (PDF No.72-0864). No peaks from other impurities were detected, which indicated that as-prepared $NbSe_2$ nanofibers had high purity.

Cr_2Nb particles, as strength phase of composites, were also characterized using XRD and SEM. Fig. 3a shows the as-prepared Cr_2Nb particles with diameters of about ~10μm. All observed diffraction peaks could be systematically indexed to Cr_2Nb (JCPDS No. 47–1639). Furthermore, element Cr peaks were detected due to Cr overdosage.

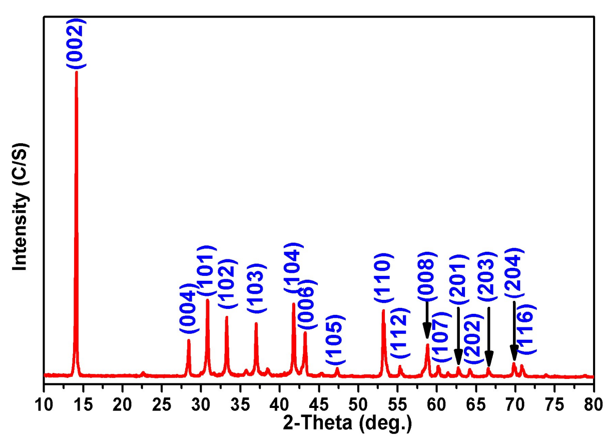

Fig.2 XRD pattern of $NbSe_2$ nanoparticles

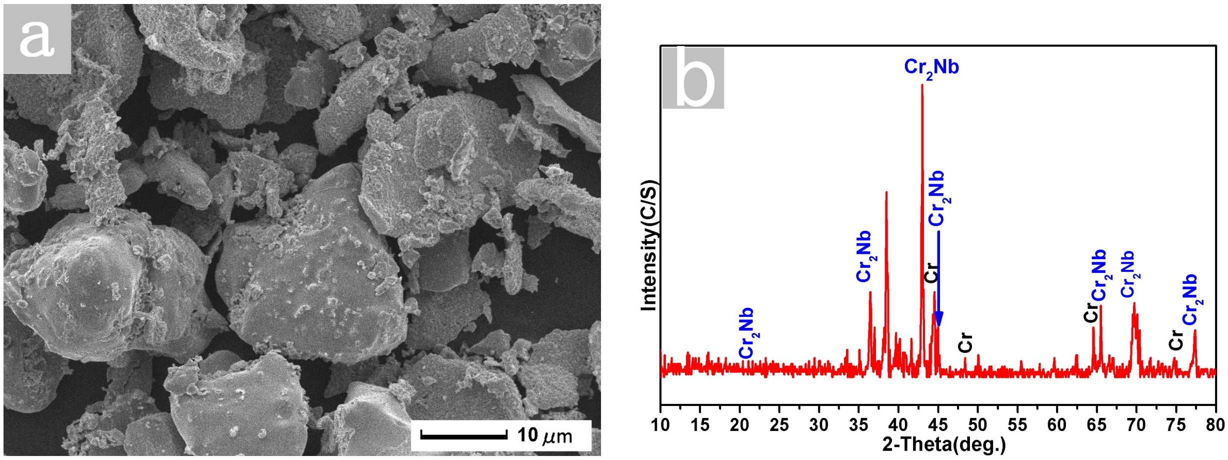

Fig.3 SEM image and XRD pattern of Cr_2Nb particles, (a) SEM image of Cr_2Nb particles, (b) XRD pattern of Cr_2Nb particles

Table 1 The chemical compositions, density and hardness of Cu-based composites in mass

specimen	Cu	Cr_2Nb	$NbSe_2$	Green density (g/cm^3)	Sintered density (g/cm^3)	Microhardness (HV)	Standard Error of Microhardness
Sa1	65	35	0	7.08	7.15	195.5	1.72
Sa2	65	25	10	7.24	7.28	176.4	1.24
Sa3	65	20	15	7.27	7.43	166.3	1.13
Sa4	65	15	20	7.34	7.47	164.3	1.47
Sa5	65	10	25	7.39	7.53	157.7	1.38
Sa6	65	0	35	7.51	7.62	83.5	1.65

3.2. Characterization, density and microhardness of Cu-based composites

The chemical compositions of Cu-based composites are shown in Table 1. Fig.4 is the XRD patterns of Cu-based composites prepared by P/M. It was found that the diffraction peaks primarily belonged to the Cu phase. Some other peaks except Cu were observed in the XRD patterns of Cu-base composites, such as Cr_2Nb and $NbSe_2$ phases as well as a small amount of newly-formed Cu_2Se and $Cu_{0.67}NbSe_2$ phases due to a complex reaction between Cu and $NbSe_2$ at high temperature. The diffraction peaks of $NbSe_2$ became stronger with the increase of the $NbSe_2$ content. However, Sa6, for sample, the diffraction peaks of $NbSe_2$ disappeared and transformed into Cu_2Se and $Cu_{0.67}NbSe_2$

phases, which might be the reason of the absence of Cr_2Nb phase. Moreover, the formation of new compounds between Cu and Cr_2Nb was not found because the high melting point intermetallic compound Cr_2Nb was not soluble in solid copper.

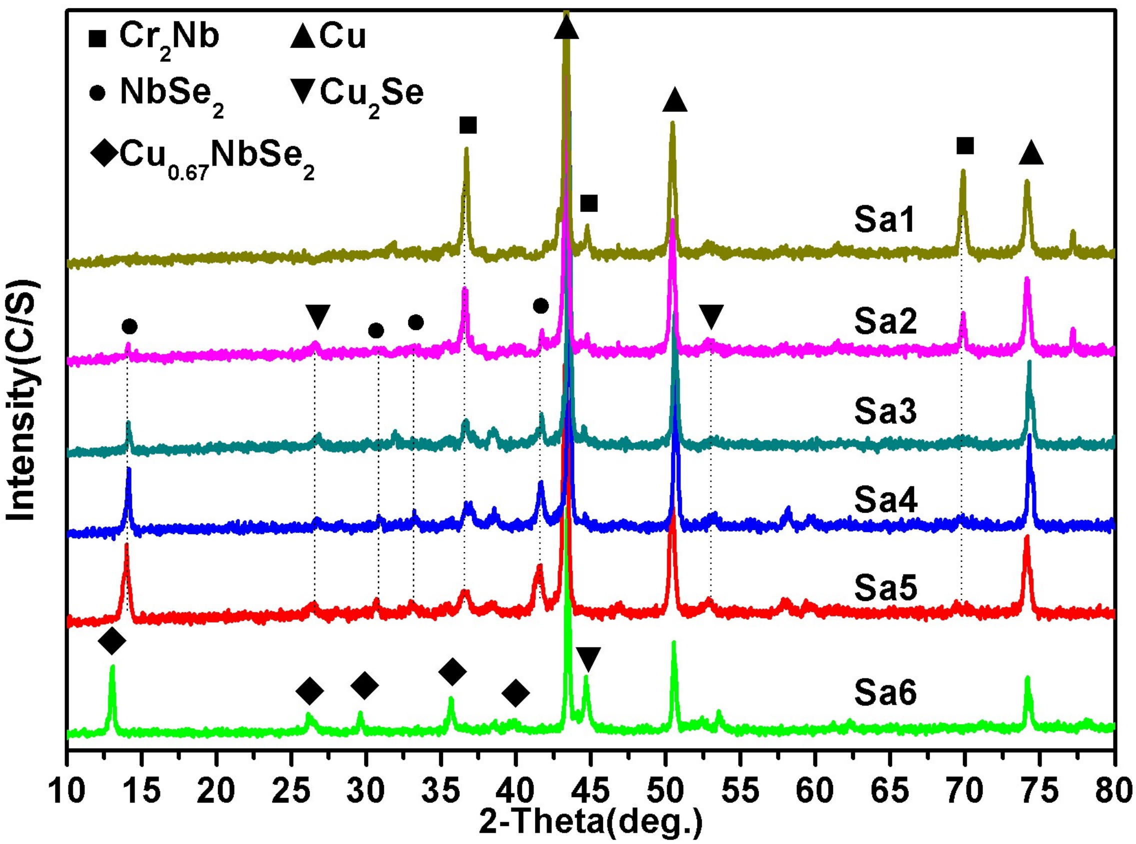

Fig.4 XRD patterns of as-prepared Cu-based composites

Fig.5a shows the XPS survey spectrum of Sa5 and Sa6, six relatively strong peaks were detected in the observed areas of the surface of the composites. The characteristic peaks of Nb, Se and Cu elements are detected for Sa5 and Sa6 in addition to some peaks of inevitable C and O elements. Moreover, the peak of Cr element is also detected for Sa5, which implies the presence of Cr_2Nb. From Fig.5b, the peak of Cu2p for Sa6 around 931.9eV is assigned to Cu^+ which suggests that copper could form Cu_2Se, and the peak of Cu2p for Sa5 around 932.6eV is assigned to Cu which suggests that copper could not react with $NbSe_2$ or Se.

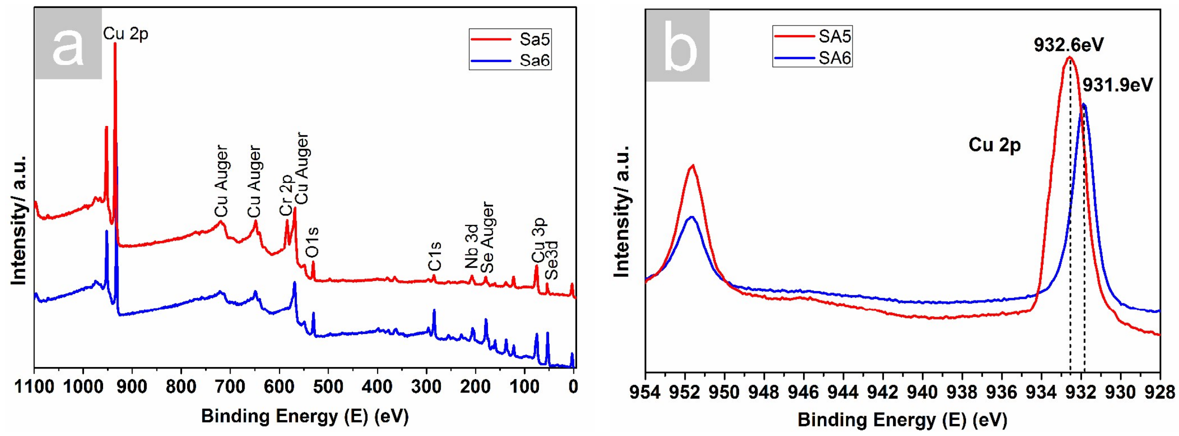

Fig.5 (a) XPS survey spectrums of sintered Sa5 and Sa6, (b) XPS spectrums of the Cu2p region of Sa5 and Sa6

Fig.6 shows the microstructure of sintered Sa1, Sa5 and Sa6 which was been characterized by Optical micrographs after metallographic preparation. The grain structures and reinforced particle's shape, size and their distribution were observed. The microstructures of $NbSe_2$ and Cr_2Nb showed good bonding of Cu particles, as indicated by the disappearance of original particle boundaries and the presence of pores. The Cr_2Nb particles embedded in the matrix and $NbSe_2$ phase along the copper phase boundaries were found in the microstructure of the Cu-based composites.

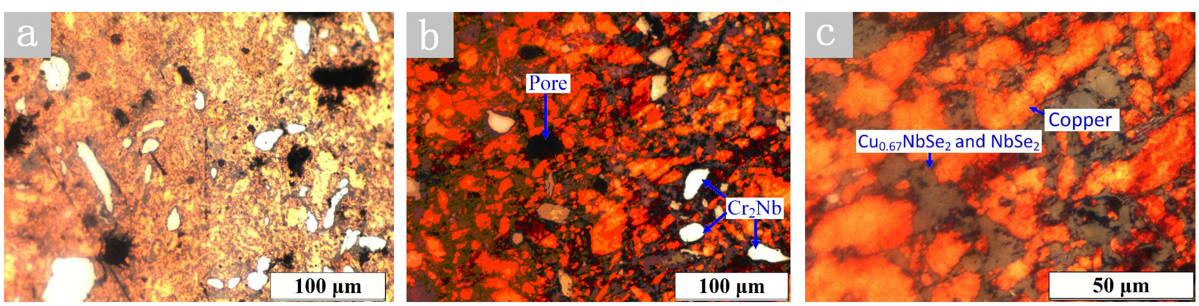

Fig.6 Optical micrographs of sintered (a) Sa1, (b) Sa5 and (c) Sa6

The density and microhardness of Cu-based composite compacts are shown in Tables 1. It could be seen that the density of Cu-based composites increased with the increasing of $NbSe_2$ contents due to higher density of $NbSe_2$ in comparison with Cr_2Nb in Cu matrix. A load of 10N and the duration time of 10s were employed for microhardness measurement. Ten tests were carried out at different places of composites and the mean value was given. The microhardness of Cu-based composites increased with the increasing of Cr_2Nb contents (Table 1), which could be ascribed to the presence of fine and uniformly distributed Cr_2Nb particles with high hardness.

3.3. Friction behavior of Cu-based composites

Fig.7a shows the relationship between friction coefficients and the loads at a sliding speed of 0.157m/s for 1200s. The error bars were the maximum and minimum values of friction coefficient among the results collected at four places on each specimen under the same experimental conditions, and the plots showed the mean values. The values of friction coefficient decrease with an increase in $NbSe_2$ content and sample Sa5 had the lowest value of friction coefficient. It also could be found that friction coefficients of composites decreased slightly at load between 1N and 3N, and further decreased to the lowest value at load of 5N. With the further increasing of load, however, the coefficients of friction tended to rise to high value. Fig.7b is friction coefficients of Cu-based composites tested at different sliding velocities (Velocity: m/s, Load: 5N, Time: 1200 s). The friction coefficients remained substantially unchanged when the sliding speed was less than 0.208m/s. However, the friction coefficients increased exponentially when the velocity was higher than 0.208m/s.

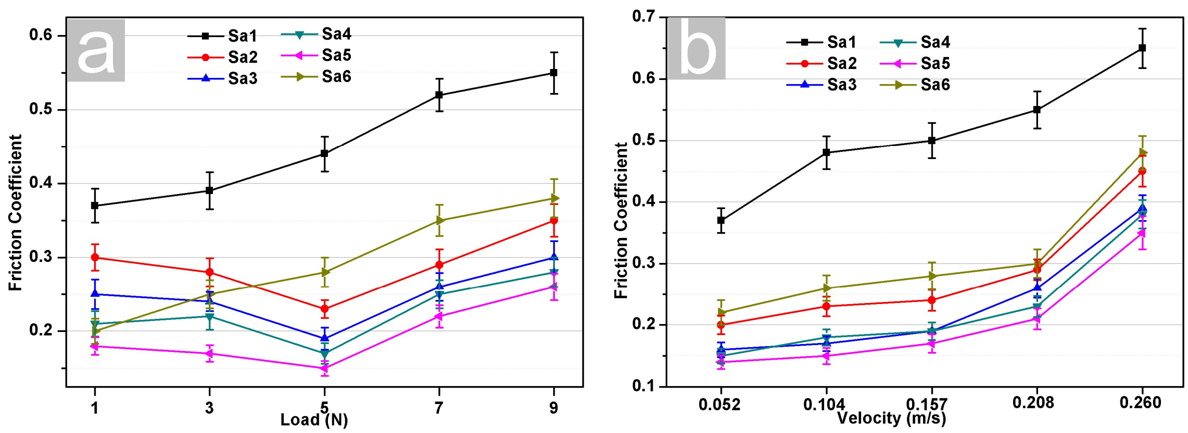

Fig.7 Friction coefficients of Cu-based composites with $NbSe_2$ nanofibiers tested at different loads and different sliding speeds, (a) Tested at different loads, (b) Tested at different sliding speeds

Fig.8 represents the friction coefficients and the wear rate of Cu-based composites in air atmosphere as a function of sliding time. The sliding speed and the applied load were set at 0.157m/s and 5N, respectively. The friction coefficients and wear rate were decreased for Cu-based composites containing $NbSe_2$ nanofibers. In the initial stage of sliding, the contact between Cu-based composites and steel ball was metal-metal because the composites contacted directly with the ball. Therefore it was obvious that the friction coefficients in the initial stage were high as shown in Fig.8a. With the time prolonged, it remained quite constant since $NbSe_2$ peeled off from the copper matrix. The lowest value for the friction coefficient was recorded for the sample Sa5 which exhibited stable sliding with a value close to 0.15, followed by Sa4, Sa3, Sa2 and Sa6. The friction coefficient of sample Sa1 remained appreciably high which might be the absence of $NbSe_2$ that functioned as solid self-lubricant in Cu-based composites.

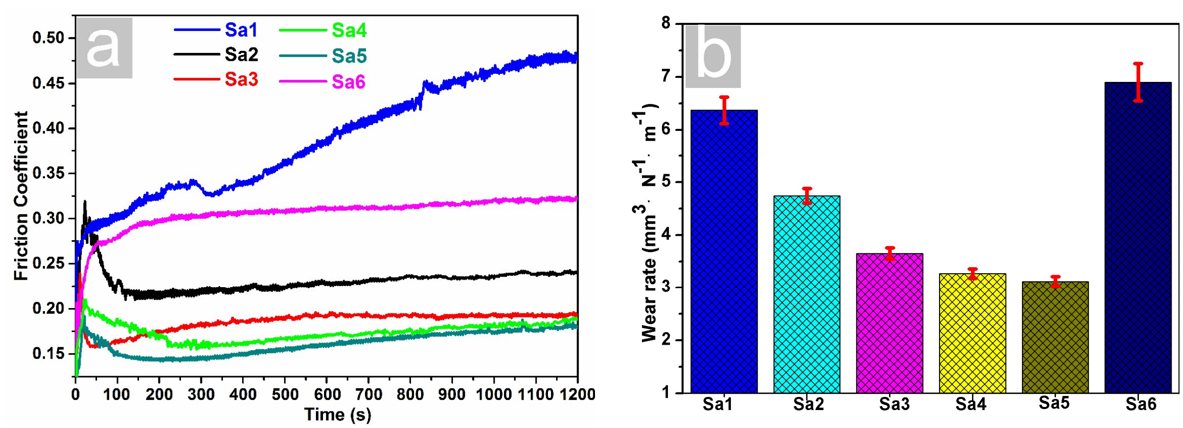

Fig.8 (a) Variation of friction coefficient of Cu-based composites, (b) Variation of wear rate of Cu-based composites

The wear rates of Cu-based composites varied with the change of Cr_2Nb and $NbSe_2$ contents, as shown in Fig.8b. The wear rate of Cu-based composites containing only $NbSe_2$ nanoparticles (sample Sa6) was highest due to the absence of Cr_2Nb particles which had high hardness, and the hardness of composites was a key factor in improving the wear resistance. Sample Sa5 had the lowest value of wear rate due to synergistic effect of $NbSe_2$ and Cr_2Nb, where $NbSe_2$ functioned as solid lubricant and Cr_2Nb as reinforcements. This result correlated very well with the recorded values of the friction coefficient.

In order to study the tribological performance of $NbSe_2$ nanofibers，another compact of Cu-based composites (sample S5) containing commercially available $NbSe_2$ micro-particles, which had the same chemical compositions in comparisons with sample Sa5, was also prepared. Fig.9 shows the variations in friction coefficients of Sa5 and S5 with the sliding speed of 0.157m/s and the applied load of 5N, respectively. From Fig.9, the friction coefficients of the Cu-based electrical contact composites with $NbSe_2$ nanofibers were much lower and more stable than those with commercially available $NbSe_2$ micro-particles in the time frame tested. The following inference might be made on the friction characteristics of these two composites with different size of $NbSe_2$ particles: $NbSe_2$ nanofibers could assist in forming lubricant layer and increase the carrying capacity of the tribo-system under dry friction conditions.

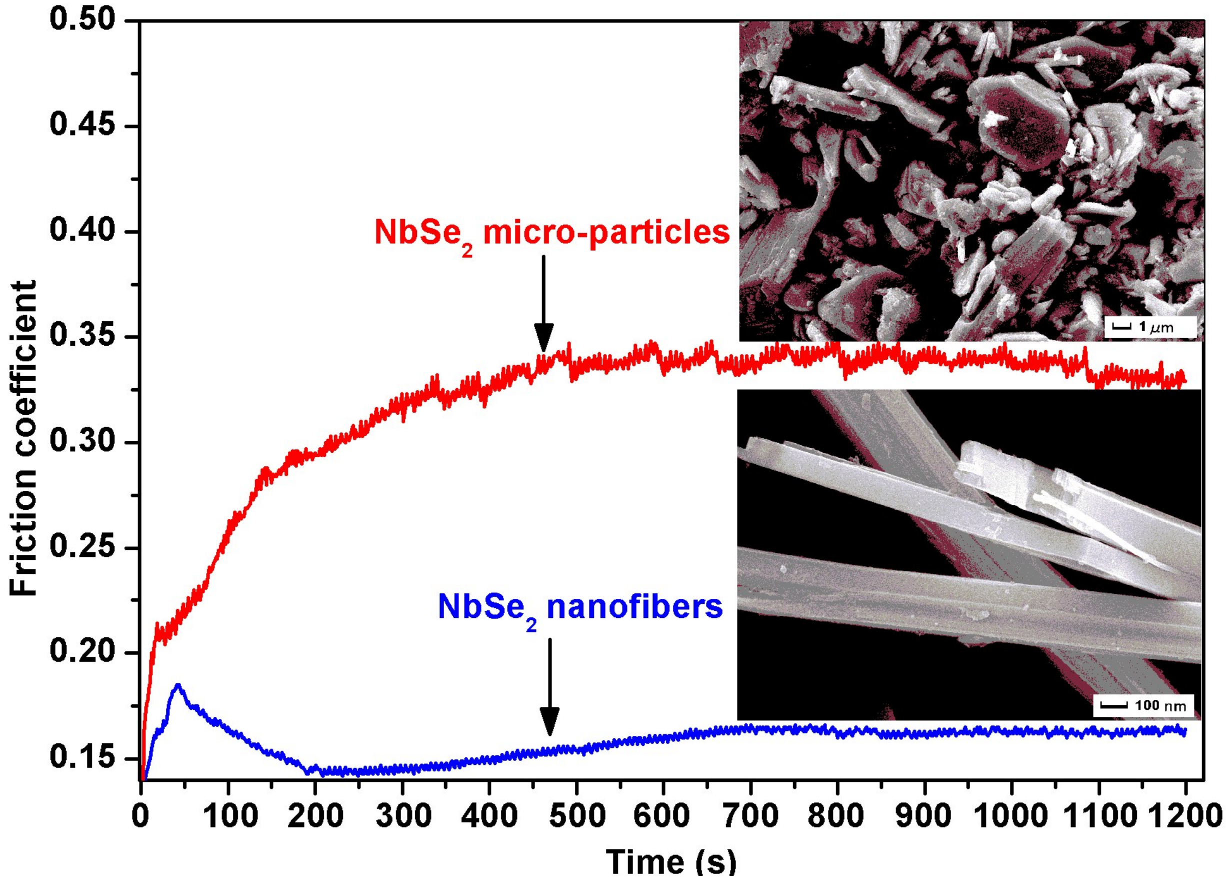

Fig.9 Variation of friction coefficient of Cu-based composites containing $NbSe_2$ nanofibers and micro-particles respectively

3.4. Wear mechanisms

The SEM images of the worn surfaces of Cu-based composites after testing under an applied load of 5N at a sliding speed of 0.157m/s are shown in Fig.10a-f. It could be found that the morphologies of worn surfaces of Cu-based composites were different with the varying of $NbSe_2$ and Cr_2Nb contents. For all samples, the asperities of surfaces underwent plastic deformation and adhesion. In addition, cracks, small frost like particles, high plastic deformation and grooves were found on the worn surface of composites.

The worn surfaces of sample Sa1 are shown in Fig.10a. Many cracks and debris were seen on the worn surface of sample Sa1. The results demonstrated abrasion and plastic deformation. In addition, many cracks were observed on the worn surface and scratches were prevented due to the presence of hard phased Cr_2Nb. With the increase in $NbSe_2$ content, however, samples Sa2, Sa3 and Sa4 suffered from defects like numerous slight grooves, delamination and a small amount of plastic deformation. The worn surface of Cu-based composites containing $NbSe_2$ particles became flat since $NbSe_2$ nanoparticles could be squeezed out from matrix, and an incomplete lubricating film could be formed because of low amount of $NbSe_2$. Fortunately, the lowest friction coefficient was found in sample Sa5 composite, whose sliding contact exhibited a smooth area with the continuous and homogenous tribo-films formed on the worn surface, as shown in Fig.10e. The films covered on the sliding surfaces changed the nature of contact from metal-metal to metal-film-metal. Moreover, a better tribological behavior of sample Sa5 was confirmed from the low value of wear rate and friction coefficient. Even though containing high level of $NbSe_2$, the worn surface of sample Sa6 was rough and an intensive plastic deformation could be seen as indicated in Fig.10f. This was due to the presence of $Cu_{0.67}NbSe_2$ compounds after sintering (Fig.4), the result of which was that the continuous and homogenous tribo-films could not be formed. The newly-formed $Cu_{0.67}NbSe_2$ compounds, in which the Cu metal atoms were located in octahedral sites in the van der Waal's gap between the layers [27], resulted in an increase in the lattice parameter c. The van der Waals interactions between Se-Se were transformed into strong covalent interactions between Se-Cu-Se due to the dissolution or intercalation of Cu into $NbSe_2$ making it difficult to shear it while being distorted. This might be the reason that sample Sa6 has a relative high friction coefficient.

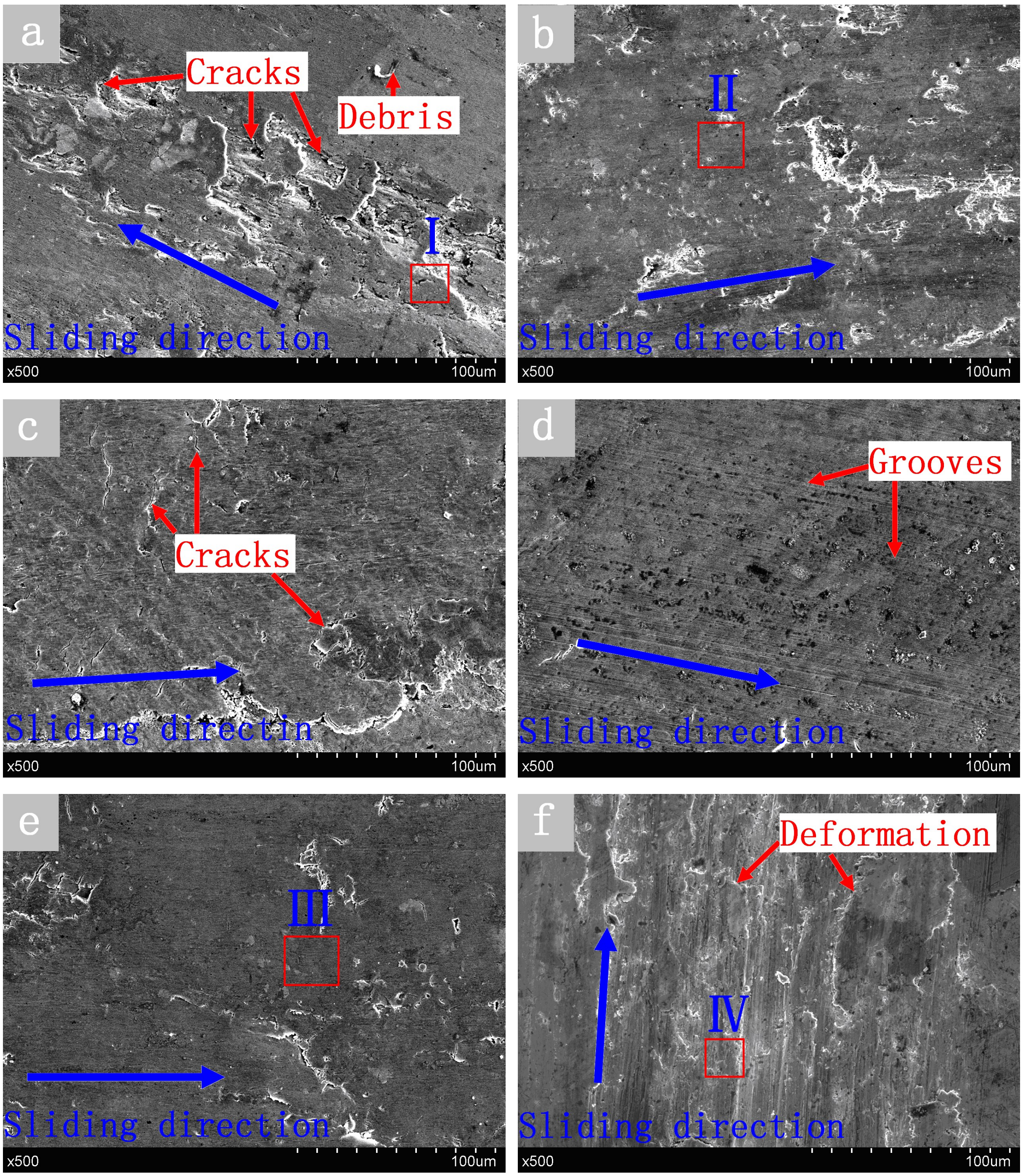

Fig.10 SEM micrographs of Cu-based composites (5N load, 188m and 0.157m/s) with different $NbSe_2$ and Cr_2Nb contents. (a)-(f) represent the worn surface of samples Sa1, Sa2, Sa3, Sa4, Sa5 and Sa6, respectively.

The EDS analysis of the area marked by a rectangle on the worn surface of samples Sa1, Sa2, Sa5 and Sa6 is shown in Fig.11. Apart from elements Nb, Cu, Cr and Se, oxygen was also observed on worn surfaces. Metallic oxide such as CuO and NbO could be formed due to the presence of oxygen. Though CuO can slightly contribute to the improvement in the tribological performance of composites [28], to a certain extent, it is known to be harmful to conductivity of electrical contact material. From Fig.11, an appreciable reduction in oxygen content of Cu-based composites was observed with the increase in Cr_2Nb content. Compared with sample Sa6, other samples had lower oxygen content due to the presence of Cr_2Nb phase which had high anti-oxidation activities. The presence of Cr_2Nb in Cu-based composites could greatly improve the wear resistance since Cr_2Nb particles were better consolidated into the Cu matrix. This might be also the reason that Sa6 had a higher wear rate as shown in Fig.8.

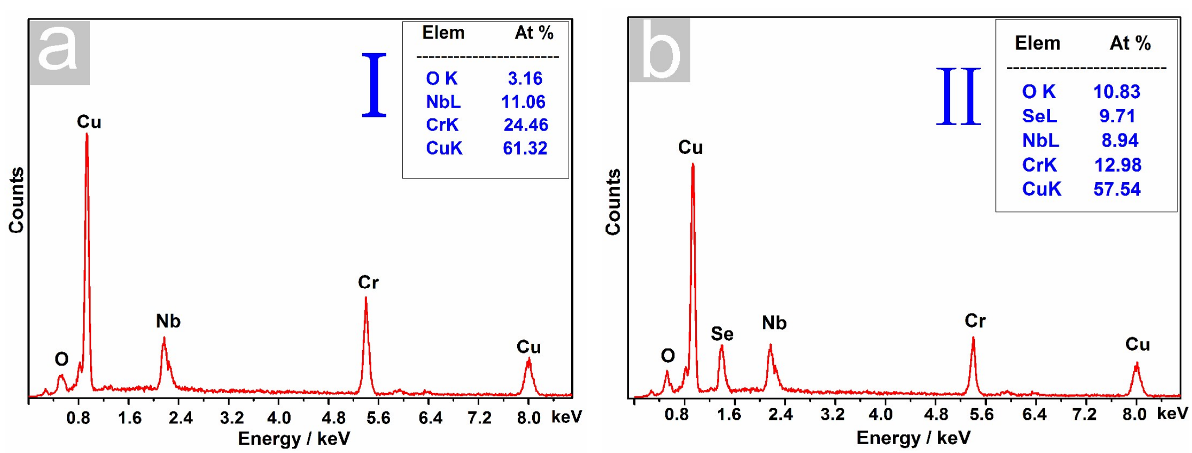

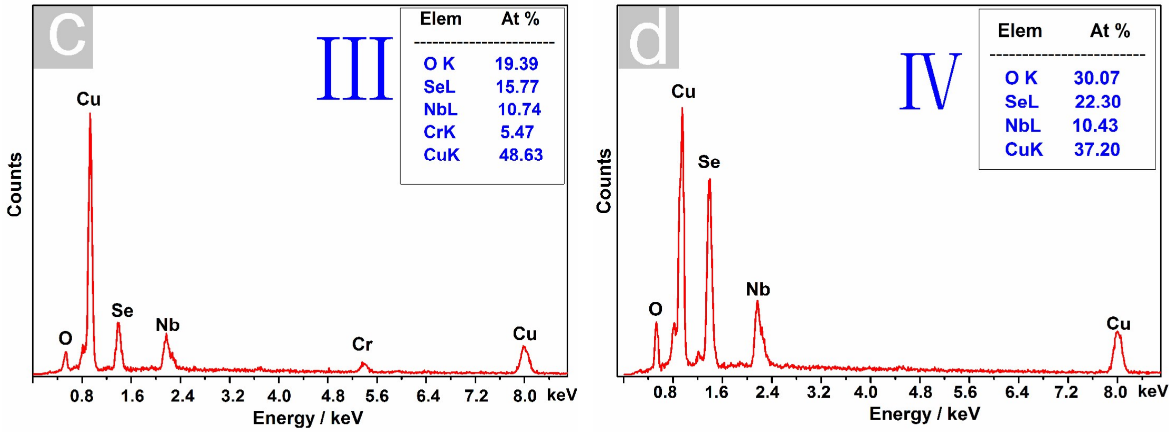

Fig.11 EDS results on the worn surface of different sample, (a)-(d) represent EDS result of samples Sa1, Sa2, Sa5 and Sa6

3.5. Electrical performance of the investigated materials

Like friction coefficient and wear rate, the electrical resistivity is also one of the main properties of the composites. As a basis for comparison, the electrical resistivity of pure copper sample which also was prepared by powder metallurgy was given in Fig.12. Though the $NbSe_2$ has higher resistivity than Copper and Cr_2Nb compounds, the overall low electrical resistivity and good conductivity of Cu-based composites are attributed to the continuous, highly conductive copper and Cr_2Nb. Fig.12 represents the electrical resistivity of Cu-based composites with different contents of $NbSe_2$ and Cr_2Nb before wearing test. The electrical resistivity increased from 5μΩ.cm to 33μΩ.cm with the increase of $NbSe_2$ contents from 0 to 20 wt%. However, further increase in $NbSe_2$ contents to 25 wt% led to an abrupt decrease in the constant value to 27μΩ.cm or 26μΩ.cm.

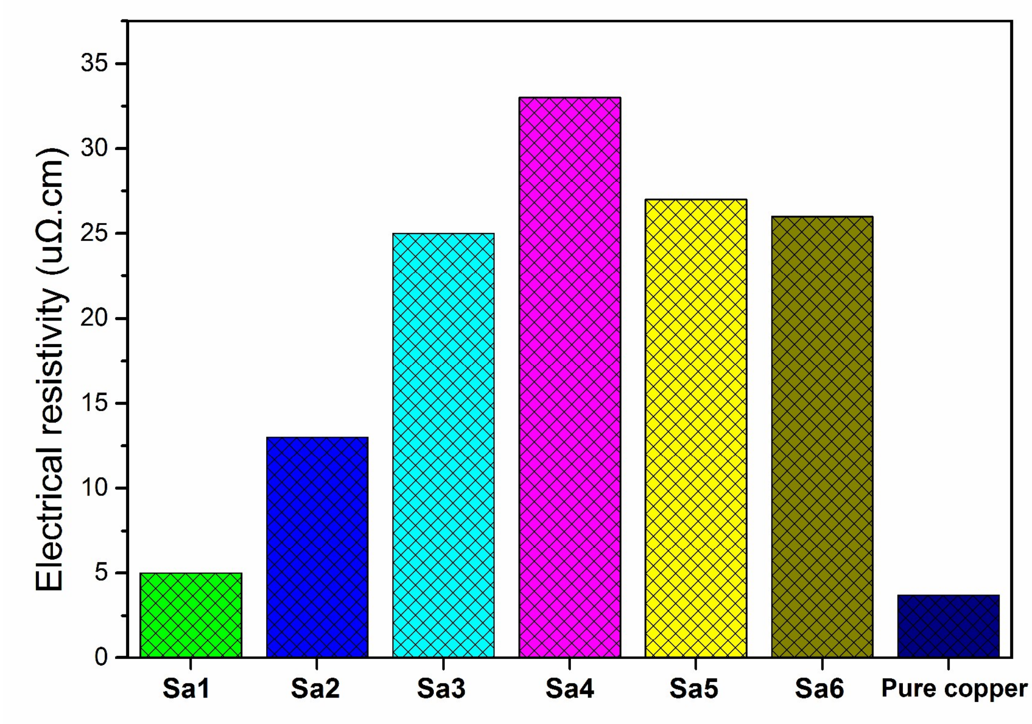

Fig.12 Electrical resistivity of pure copper and Cu-based composites with different contents of $NbSe_2$ and Cr_2Nb

The electrical resistivity increased first and then decreased before wearing test. There might be two reasons for this behavior: one was the formation of CuO which could impair the conductivity of Cu-based composites; another was the reaction of a small amount of $NbSe_2$ components with copper, as well as the presence of newly-formed Cu_2Se and $Cu_{0.67}NbSe_2$ compounds. From Fig. 4, the Cu_2Se peak weakened slightly and $Cu_{0.67}NbSe_2$ peak strengthened gradually with the increase of $NbSe_2$ contents. The newly-formed Cu_2Se compound was a semi-conducting material which could seriously impair the conductivity of composites. However, the conductivity of $Cu_{0.67}NbSe_2$ compounds was reasonably high, which was perhaps attributed to the chains of metal atoms Nb-Cu-Nb-linking through the layers. Therefore, Cu-based composites containing both Cr_2Nb and $NbSe_2$ had excellent electrical and tribological properties due to the synergetic effect Cr_2Nb and $NbSe_2$.

4. Conclusions

In this paper, a new type of Cu/Cr_2Nb/$NbSe_2$ composites was presented and their mechanical, tribological and electrical properties were assessed. The main results and conclusions of this paper could be summarized as follows:

(1) The addition of $NbSe_2$ increased the density of composites, while the addition of Cr_2Nb improved the hardness of Cu-based composites.

(2) The friction coefficient of Cu-based composites only containing Cr_2Nb (sample Sa1) in steady state was about 0.5. Sample Sa6 containing 35 wt% of $NbSe_2$ had a higher friction coefficient than other samples since intercalation of Cu into $NbSe_2$ transformed Van der Waals interactions between Se-Se into the strong covalent interactions between Se-Cu-Se. However, the friction coefficients of Cu-based composites containing both $NbSe_2$ and Cr_2Nb particles decreased with the increase of $NbSe_2$ content and sample Sa5 had the lowest value of about 0.15. Furthermore, the tribological properties of the Cu-based electrical contact composites with $NbSe_2$ nanofibers were better than those with commercially available $NbSe_2$ micro-particles.

(3) The wear rate decreased first and then increased with the increasing of $NbSe_2$ content. Sample Sa5 also had the lowest wear rate due to synergistic effect of $NbSe_2$ and Cr_2Nb, where $NbSe_2$ and Cr_2Nb functioned as solid lubricant and reinforcements, respectively.

(4) The reduced electrical resistivity of Cu-based composites was resulted from the increase of Cr_2Nb content and the formation of $Cu_{0.67}NbSe_2$ compounds. The Cr_2Nb compound had high conductivity and anti-oxidation activities and newly-formed $Cu_{0.67}NbSe_2$ had the chains of metal atoms Nb-Cu-Nb-linking through the layers.

Acknowledgements

This work was financially supported by National Natural Science Foundation of China (51275213, 51302112), the Jiangsu National Nature Science Foundation (BK2011534, BK2011480), the Scientific and Technological Innovation Plan of Jiangsu Province in China (Grant Nos. CXLX13_645,

CXZZ13_0669, KYLX_1029).

References

[1]S.G. Jia, P. Liu, F.Z. Ren, B.H. Tian, M.S. Zheng, G.S. Zhou, Sliding wear behavior of copper alloy contact wire against copper-based strip for high-speed electrified railways, Wear 262(2007) 772-777.

[2]S. Biyik, F. Arslan, M. Aydin, Arc-Erosion Behavior of Boric Oxide-Reinforced Silver-Based Electrical Contact Materials Produced by Mechanical Alloying, J. Electron. Mater. 44(2015) 457-466.

[3]X. Qiao, Q. Shen, L. Zhang, C. Lawson, X. Fan, H. Yang, A Novel Method for the Preparation of Ag/SnO_2 Electrical Contact Materials, Rare Metal Mat. Eng. 43(2014) 2614-2618.

[4] B. Ma, Q. Li, L. Li, G. Huang, L. Cheng, S. Xie, Effects of Duplex Aging on Microstructure and Properties of High-Strength and High-Conductivity Cu-Cr-Zr Alloys, Rare Metal Mat. Eng. 412(2012) 339-342.

[5]P. Zhang, J. Jie, H. Li, T. Wang, T. Li, Microstructure and properties of TiB2 particles reinforced Cu-Cr matrix composite, J. Mater. Sci. 50(2015) 3320-3328.

[6]Y. Watanabe, High-speed sliding characteristics of Cu-Sn-based composite materials containing lamellar solid lubricants by contact resistance studies, Wear. 264(2008) 624-631.

[7]Z. Wang, Y. Zhong, X. Rao, C. Wang, J. Wang, Z. Zhang, W. Ren, Z. Ren, Electrical and mechanical properties of Cu-Cr-Zr alloy aged under imposed direct continuous current, T. Nonferr. Metal. Soc. 22(2012) 1106-1111.

[8]M. Grandin, U. Wiklund, Friction, wear and tribofilm formation on electrical contact materials in reciprocating sliding against silver-graphite, Wear. 302(2013) 1481-1491.

[9]S.G. Jia, P. Liu, F.Z. Ren, B.H. Tian, M.S. Zheng, G.S. Zhou, Electrotribological property of the Cu-Ag-Cr alloy with high-strength and high-conductivity, Met. Mater. Int. 13(2007) 25-30.

[10]S. Lu, C. Hu, K. Wang, X. Li, X. Xiao, Y. He, The Microstructures and Properties of Novel-Type Cu/Cr_2Nb Contact Materials Fabricated Mechanically Activated Hot-Pressing, Rare Metal Mat. Eng. 38(2009) 842-846.

[11]T. Larionova, T. Koltsova, Y. Fadin, O. Tolochko, Friction and wear of copper–carbon nanofibers compact composites prepared by chemical vapor deposition, Wear, 319(2014) 118-122.

[12]A. Kellou, T. Grosdidier, C. Coddet, H. Aourag, Theoretical study of structural, electronic, and thermal properties of Cr_2(Zr,Nb) Laves alloys, Acta Materialia. 53 (2005) 1459-1466.

[13]A.K. Shukla, S.V.S.N. Murty, S.C. Sharma, K. Mondal, Aging behavior and microstructural stability of a Cu-8Cr-4Nb alloy, J. Alloy. Compd. 590(2014) 514-525.

[14]P.S. Kumar, K. Manisekar, E. Subramanian, R. Narayanasamy, Dry Sliding Friction and Wear Characteristics of Cu-Sn Alloy Containing Molybdenum Disulfide, Tribol. T. 56(2013) 857-866.

[15]X. Zhang, D. Zhang, H. Tang, X. Ji, Y. Zhang, G. Tang, C. Li, Facile synthesis and characterization of hexagonal NbSe2 nanoplates, Mater. Res. Bull. 53(2014) 96-101.

[16]G. Tang, J. Zhang, C. Liu, H. Tang, C. Li, Facile synthesis of single-crystal $NbSe_2$ ultrathin nanosheets via a pressureless sintered process, Mater. Lett. 124(2014) 289-292.

[17]H. Tang, K. Cao, Q. Wu, C. Li, X. Yang, X. Yan, Synthesis and tribological properties of copper matrix solid self-lubricant composites reinforced with $NbSe_2$ nanoparticles, Cryst. Res. Technol. 46(2011) 195-200.

[18]L. De Los Santos Valladares, D. Hurtado Salinas, A. Bustamante Dominguez, D. Acosta Najarro, S.I. Khondaker, T. Mitrelias, C.H.W. Barnes, J. Albino Aguiar, Y. Majima, Crystallization and electrical resistivity of Cu_2O and CuO obtained by thermal oxidation of Cu thin films on SiO_2/Si substrates, Thin Solid Films. 520(2012) 6368-6374.

[19]Z.L. Hu, Z.H. Chen, J.T. Xia, Study on surface film in the wear of electrographite brushes against copper commutators for variable current and humidity, Wear. 264(2008) 11-17.

[20]Z. Hu, Z. Chen, J. Xia, G. Ding, Effect of PV factor on the wear of carbon brushes for micromotors, Wear. 265(2008) 336-340.

[21]S. Hong, C.L. Fu CL, Phase stability and elastic moduli of Cr_2Nb by first-principles calculations, Intermetallics, 7(1999) 5-9.

[22]K. Li, S. Li, Y. Xue, H. Fu, Microstructure characterization and mechanical properties of a Laves-phase alloy based on Cr_2Nb, Int. J. Refract. Met. H. 36(2013) 154-161.

[23]W. Li, L. Hu, M. Wang, H. Tang, C. Li, J. Liang, Y. Jin, D. Li, Synthesis and tribological properties of Mo-doped WSe_2 Nanolamellars, Cryst. Res. Technol. 47(2012) 876-881.

[24]G. P. Khanra, A. K. Jha, S. Girikumar, K. T. Tharian, S. Kumar, Processing of Cr_2Nb precursor through powder metallurgy route, Powder Technol. 197(2010) 177-183.

[25]H. Ashuri, A. Hassani, Characterization of severely deformed new composites fabricated by powder metallurgy including a stage of mechanical alloying, J. Alloy. Compd. 617(2014) 444-454.

[26]V.S. Mironov, J.K. Kim, M. Park, S. Lim, W.K. Cho, Comparison of electrical conductivity data obtained by four-electrode and four-point probe methods for graphite-based polymer composites, Polym. Test. 26(2007) 547-555.

[27]T. Ohtani, A. Tsubota, K. Ohshima, Intercalation of copper into some layered and tunnel chalcogenides by mechanical alloying, Mater. Res. Bull. 34(1999) 1143-1152.

[28] A. T. Battez, J. L. Viesca, R. González, Friction reduction properties of a CuO nanolubricant used as lubricant for a NiCrBSi coating, Wear. 268(2010) 325-328.

[29]W. C. Zapata, C. E. Da Costa, J. M. Torralba, Sinterability and wear behaviour of P/M M2 high speed steel reinforced with NbC composite, J. Mater. Process. Tech. 53(1995) 483-490.

[30]S. Mahathanabodee, T. Palathai, S. Raadnui, Effects of hexagonal boron nitride and sintering temperature on mechanical and tribological properties of SS316L/h-BN composites, Materials & Design, 46(2013) 588-597.

[31]M. D. Abad, J. C. Sanchez-Lopez, Tribological properties of surface-modified Pd nanoparticles for electrical contacts, Wear. 297(2013) 943-951.

[32]A. M. Kovalchenko, O. I. Fushchich, S. Danyluk, The tribological properties and mechanism of wear of Cu-based sintered powder materials containing molybdenum disulfide and molybdenum diselenite under unlubricated sliding against copper, Wear. 290(2012) 106-123.